Non-Intrusive Geo-Electrical ERT Monitoring of High-Level Radioactive Waste Experiments in Tournemire URL

Bruna De Carvalho Faria Lima Lopes[1*], Pierre Dick[2], Johan Bertrand[3] José Luis García-Siñeriz[4] & Alessandro Tarantino[1]

[1] University of Strathclyde, Scotland, United Kingdom.
[2]Institut de Radioprotection et de Sûreté Nucléaire, France
[3]Agence Nationale Pour La Gestion Des Déchets Radioactifs, France
[4]AMBERG Infraestructura, Spain
* Corresponding Author, E-mail: bruna.lopes@strath.ac.uk

Summary
Geophysical electrical resistivity tomography (ERT) is a promising measurement technique for nonintrusive monitoring of an engineered barrier system (EBS) of geological disposal of high-level radioactive waste. Electrical resistivity is sensitive to water content and temperature, which are the key variables characterizing the response of the EBS. In order to assess the technology readiness level of the ERT technique for EBS operational monitoring, ERT survey campaigns have been carried out in two field demonstrator developed at the underground research laboratory (URL) in Tournemire (France) within the project 'Modern 2020', called ERT experiment and LTRBM. Preliminary ERT surveys were carried out to establish the background resistivity of the experimental areas and assess the quality of electrode installation and survey protocols. Monitoring ERT surveys are underway after the installation of both experiments in July 2018 (LTRBM) and September 2018 (ERT experiment). Results of firsts blank test surveys carried out on both experiments confirmed that the resistivity of the host rock around both experiments area is quite homogenous and lower than 100Ωm. Preliminary results of the monitoring period for both experiments are also promising, different materials within the installation are identifiable and changes in resistivity due to water injection and temperature increase are also expected to be noticeable.

1. Introduction

Current radioactive waste management programmes in most countries are focused on disposal of long-lived waste in geological repositories as the most appropriate approach to ensure long-term safety of people and the environment [1]. The combination of a selected host rock and an Engineered Barrier Systems (EBS) to protect and isolate the waste is considered in almost all programmes. A swelling clay is generally used in the EBS as a buffer that surrounds and protects the individual waste packages and/or to seal off the disposal galleries from the shafts leading to the surface. Understanding of the clay barriers behaviour in time is fundamental for a final repository

for high-level radioactive waste to be granted license. Therefore, monitoring the EBS could be required to help assessing its proper performance.

During the maturing phase of buffer materials in deep geological repository, water saturation and temperature are two key parameters that have been mentioned in every international collaborative work on monitoring strategies and parameters selection. The EBS is subjected to an inwards water flow from the host rock and an outwards heat flux from the radioactive waste. Changes in water content and temperature are therefore the key to assessing the performance of the EBS. EBS monitoring using wired sensors installed in the buffer should be avoided because wires could provide a preferential pathway for radionuclide leakage as well as for water [2]. Geophysical electrical monitoring is potentially an ideal technique for geophysical diffuse monitoring of the EBS because: (i) it can be designed in a less-intrusive fashion; (ii) it allows local anomalies to be captured that local sensors cannot spot; and (iii) electrical resistivity is very sensitive to changes in water content and temperature, and is therefore very convenient to monitor the EBS [3–9].

Electrical resistivity tomography (ERT) is a well-established geophysical technique that uses the injection of electrical currents and measurements of the resulting voltage differential at the Earth's surface or in boreholes. This generates pseudo-sections displaying apparent resistivity as a function of the location and electrode spacing, which in turn provides an initial picture of the resistivity distribution. An inversion process of the measured data is necessary for the final interpretation of the resistance data. This process transforms the apparent resistivity into 2D or 3D images of the bulk electrical resistivity of the subsurface model, which is discretized into a distinct number of elements of homogeneous resistivity.

ERT surveys have been routinely used in water exploration and contaminant flow detection [10–15], engineering site investigations [16–20], and in the location of buried artefacts or structures in archaeological surveys [21–24] as well as providing geological and hydrogeological site information [25–27]. ERT in boreholes has proven useful for environmental investigations [28–34]. The method has also been demonstrated to be economically efficient when using wells drilled for geotechnical pre-investigation tunnelling sites to obtain information about the geology between the wells [35]. More recently, investigations using ERT in boreholes have been extended to a variety of other applications such as the characterization and monitoring of water infiltration [5–36–37], and in monitoring CO_2 migration [38–39].

Previous researches conducted in repository-like conditions have demonstrated the potential of ERT in monitoring the EBS. ERT [40] could detect the water intake in an experiment conducted in an area at the Aespoe Hard Rock Laboratory (HRL) in Sweden. ERT electrode arrays were installed in the backfill, buffer and rock, and the water saturation changes in those three structures were monitored for a few years. Similarly, the EB Experiment [41] used ERT electrode arrays installed in the Engineered Barrier Emplacement Experiment in Opalinus Clay at the Mont Terri underground laboratory in Switzerland. Several ERT surveys were conducted over the 11 years of operation of the experiment to monitor water intakes in different areas of the experiment. However, in all these experiments, the ERT electrodes were buried inside the EBS and this arrangement is less suitable for long-term monitoring of the EBS in the repository. To the best of the authors' knowledge, there has been no attempt to date to investigate the use of the ERT technique in a non-intrusive fashion: that is, with the electrodes positioned outside the buffer.

This paper presents preliminary results of the ERT monitoring surveys carried out in two scale tests installed at the underground research laboratory (URL) in Tournemire (France), known as the ERT experiment and the Long Term Rock Buffer Monitoring (LTRBM).

2. Methodology

2.1. Experiments overview

The ERT experiment was purposely designed to assess the capabilities of ERT as a non-intrusive technique of monitoring the EBS under conditions as close as possible to the ones expected in the real repository, while the LTRBM was designed to asses the capabilities of new monitoring devices, mainly wireless devices including long term power supply solutions and new sensors, developed within 'Modern2020' project.

The installation of the ERT experiment took place between June and September 2018, and the installation of the LTRBM took place between June and July 2018, an overview of both experiments are shown in Figure 1. Local sensors were installed into the EBS in both experiments to measure water content (and temperature for the ERT experiment only) as a way of cross-checking the geophysical measurements. For research purposes, electrodes were also buried inside the main shaft in the ERT experiment. Unfortunately, one line of electrodes is malfunctioning since after the installation, a damage most probably caused during the installation activities. After curing of the cement plug, September and October 2018 for the LTRBM and ERT experiment respectively, hydration (and heater tests for the ERT experiment only) started together with scheduled ERT monitoring surveys. A summary of the test's characteristics are presented in Table 1.
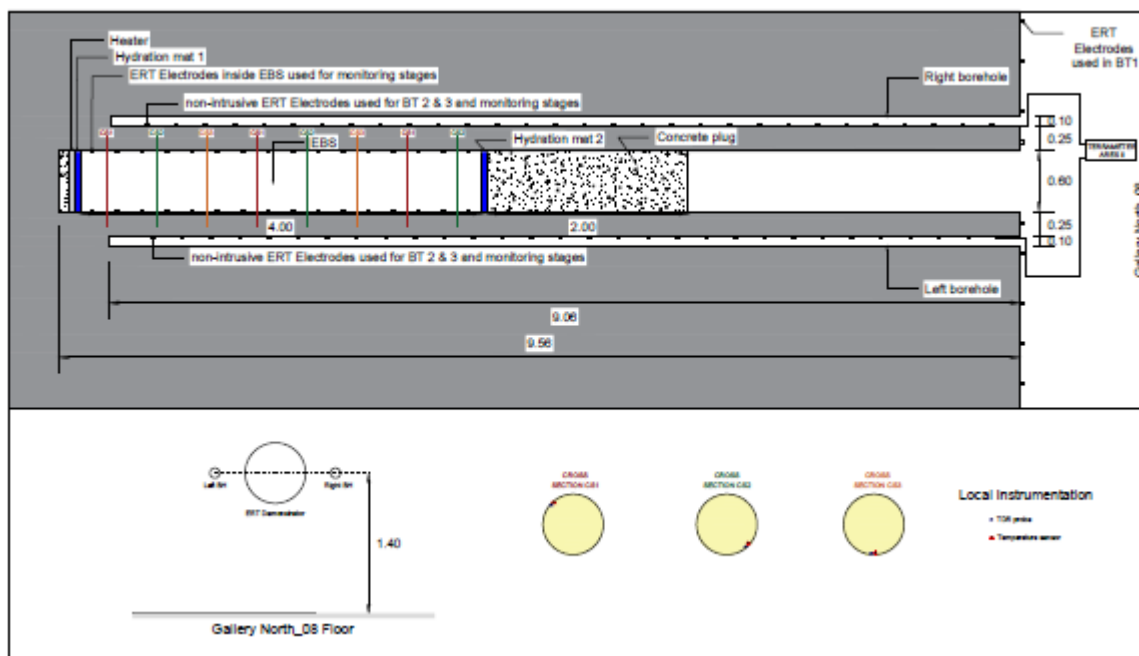
(a)
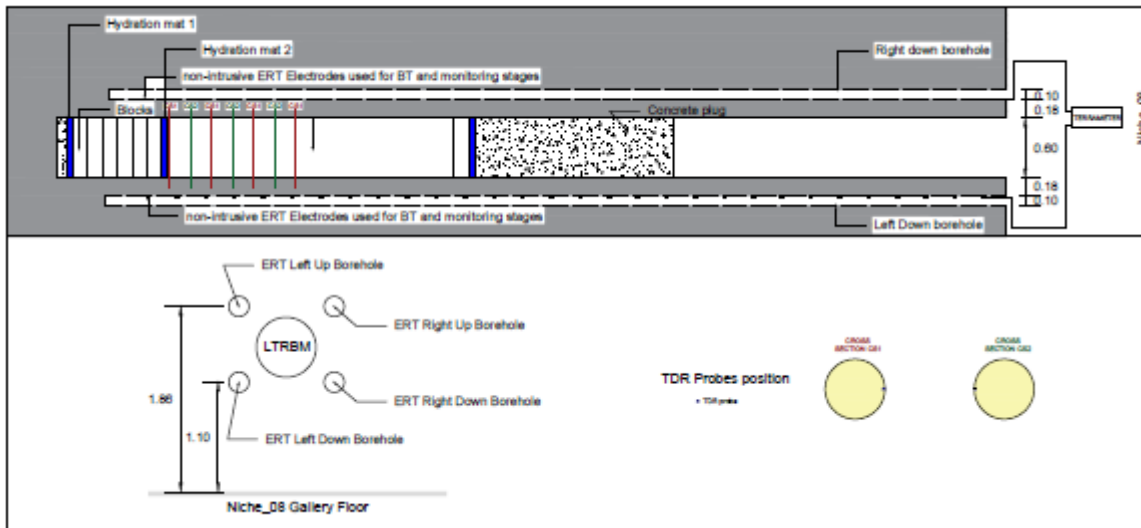
(b)

Figure 1 Overview of (a) ERT experiment and (b) LTRBM

Table 1 : Summary of tests characteristics

Characteristics/ test	ERT Experiment	LTRBM
No. of ERT boreholes	2: One on either side of Main shaft	4: forming an x around the main shaft
No. of Non-intrusive ERT electrodes	64: 32 in each borehole (0.29m spacing)	128: 32 in each borehole (0.27m spacing)
No. of ERT electrodes inside buffer	32: 2 parallel lines of 16 each (0.24m spacing)	None
Blank tests: to measure rock background resistivity	S1 & S2 (Jan 2017) and S3 (Nov 2017)	T1 (Feb 2018)
Size of Main Shaft	Diameter: 0.60m Length: 9.54m	Diameter: 0.60m Length: 9.50m
Installation	June–September 2018	June-July 2018
Length of EBS	4m	4m
Material of EBS	Bentonite pellets and powder [42]	Highly compacted bentonite blocks (HCBB) & 60% Bentonite pellets + 40% Sand (GM)
Local Instrumentation installed inside EBS	8 TDR probes and 8 Temperature sensors	7 TDR probes* within GM
Length of cement plug	2m	2m
Hydration mats	2: one in each end of EBS	5: One in both ends of the EBS, one in the transition between the HCBB and the GM and the last two mats were installed radially around the main shaft in the area of the GM
Heater	Rear of the EBS	None
Hydration started	October 2018	September 2018
Heating started	October 2018	Not possible

* Several other local sensors were installed in the LTRBM, but only TDR probes are worth mentioning for the purposes of this paper.

The non-intrusive ERT electrodes used on both experiments were mounted in PVC tubes at a fixed distance and installed into boreholes drilled in the rock. Usually, water is added within the borehole to ensure contact in these surveys. However, this resource is not an option for the ERT demonstrator and LTRBM experiments since the electrode boreholes in question are horizontal. It is not possible to keep water in horizontal boreholes, thus continuous injection of water would be necessary in this situation, which would perturb the experiment. Consequently, a system described in [43] which injects compressed air in an inflatable balloon at the back of the PVC pipes is used to improve contact between the electrodes and the rock walls. Despite these measures contact resistance is still one of the main concerns which surrounds the surveys on both experiments.

2.2. ERT surveys

Three preliminary ERT surveys were carried out on the ERT experiment area in January and November 2017 before the emplacement of the bentonite, while a preliminary ERT survey was carried out in February 2018 on the LTRBM area before the installation of the buffer. These surveys were aimed at a first assessment of the electrode installation technique, ERT measurement protocols and inversion procedures. Due to restrains of space, we are presenting here two surveys performed on the ERT experiment area and two surveys performed on the LTRBM area, as described in Table 2.

Table 2: ERT surveys performed on ERT experiment and LTRBM area presented in this paper

Survey context	ERT experiment	LTRBM
Blank test	S2	T1
Monitoring stage	S6	T2

Terrameter LS, manufactured by ABEM was used for the data collection of all ERT surveys presented in this report.

Overall, contact resistance, stacking errors and reciprocal measurement errors (for S6 and T2) were the three features used to filter the data collected in the surveys performed. Details on data collection and quality procedure can be seen in [43].

All inversions carried out on the ERT experiment and LTRBM were performed using Res2DInv [44] and Res3DInv [45] respectively. The inversion method used was the L1 norm to account for data sets containing non-random noise.

3. Results

3.1. ERT experiment

Survey S2 occurred in January 2018 and was a combination of data collected from arrays involving in-hole and crosshole quadripole combinations. The data were processed in cross-borehole format, treated in terms of contact resistance and stacking errors and inverted. Figure 2 shows that the resistivity between the two boreholes is somehow homogeneous and less than 100 Ωm. The area of higher resistivity around the electrodes and in the middle of the model (around 5 m depth) is most likely to be due to artefacts created by the noise survey. Figure 3 shows the ERT inversion of

survey S6 performed during the monitoring stage in late October 2018. The data for S5 survey were processed, treated in terms of contact resistance, stacking errors and reciprocal errors and inverted.
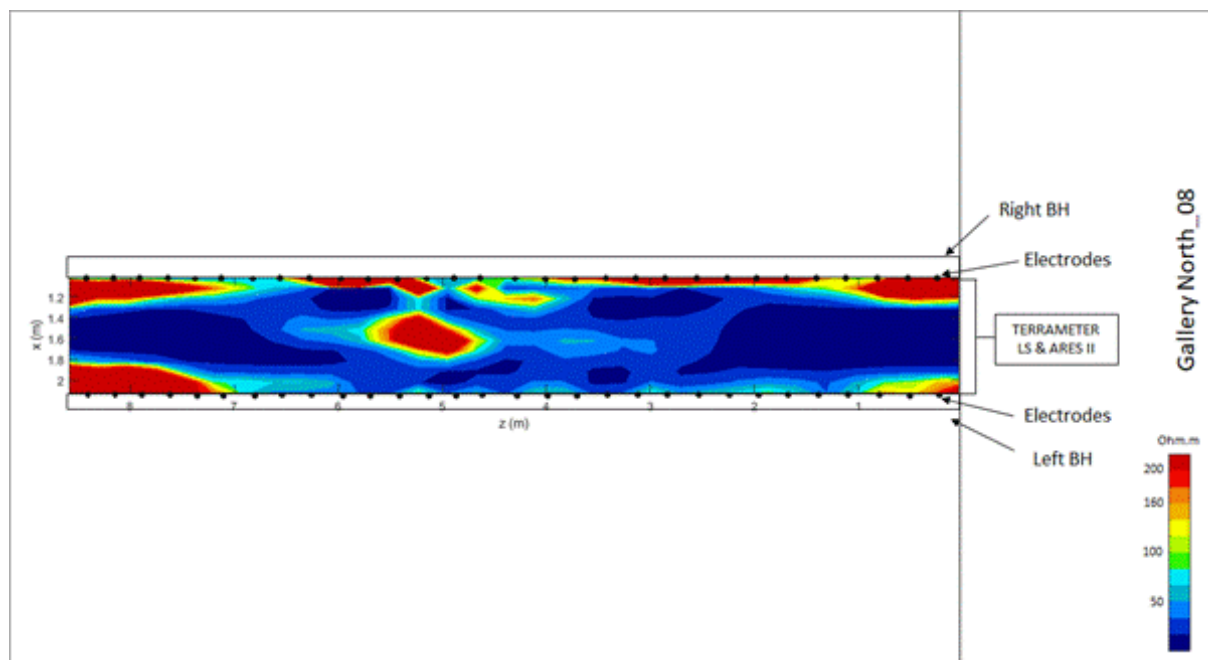

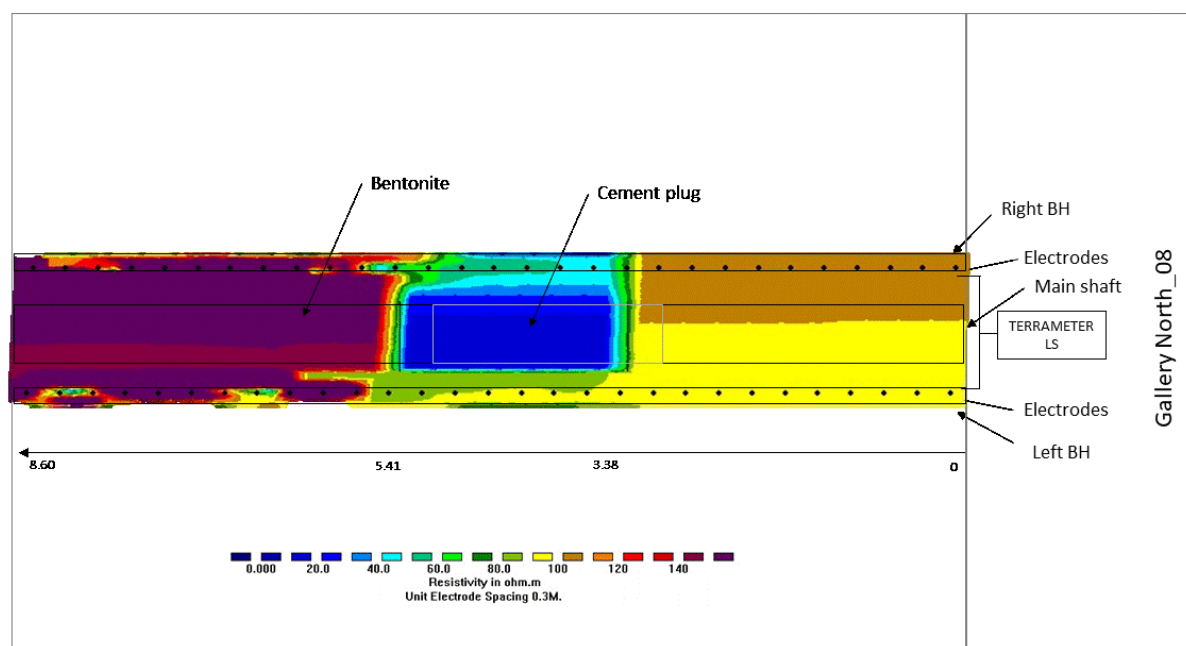*Figure 2: Cross borehole Survey S2 (RMS = 12.7%)*

Figure 3: Cross borehole survey S6 (RMS = 1.1%)

It is worth noting that the resistivity shown in survey S6, from depths 0 to 3.4m are not real. The sensitivity in this region was deliberately low in the protocol used in this survey as it envelops the empty shaft of the MB, which is not the area of interest here. Survey S6 distinguishes well the area of the cement plug and the bentonite. Additionally, it seems to be able to detect the narrow rock section between the shaft and electrodes boreholes around the cement plug section but not around the bentonite section. This is a consequence of the high resistivity of the dry bentonite material.

3.2. LTRBM

The data for T1 survey were processed, treated in terms of contact resistance and stacking errors and inverted. The inversion model of survey T1 (Figure 4 and Figure 5) shows that the resistivity between the boreholes area is somehow homogeneous and around 100 Ωm which is consistent with the blank test results obtained in the ERT demonstrator area (S2). In the models below, z is the depth axis of the buffer and xy is the cross section plane from the gallery Niche_08.
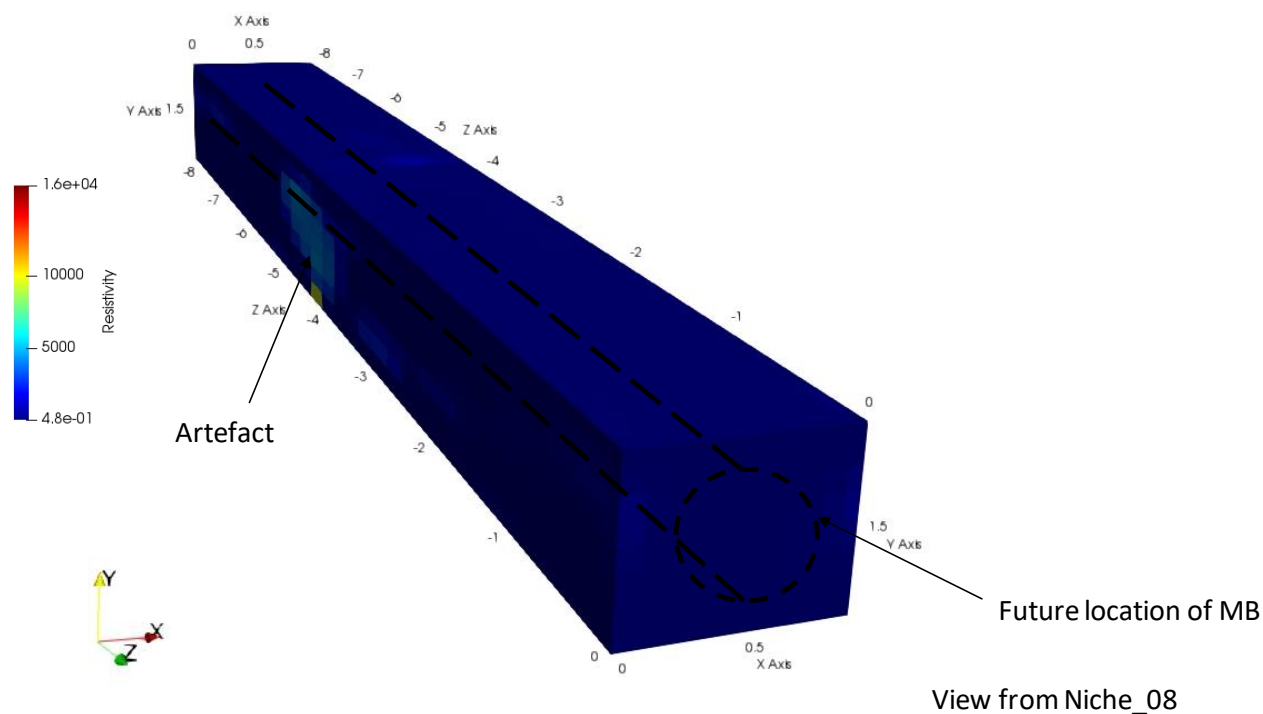

Figure 4: 3D view of inversion results from survey T1 (RMS = 10.7%)
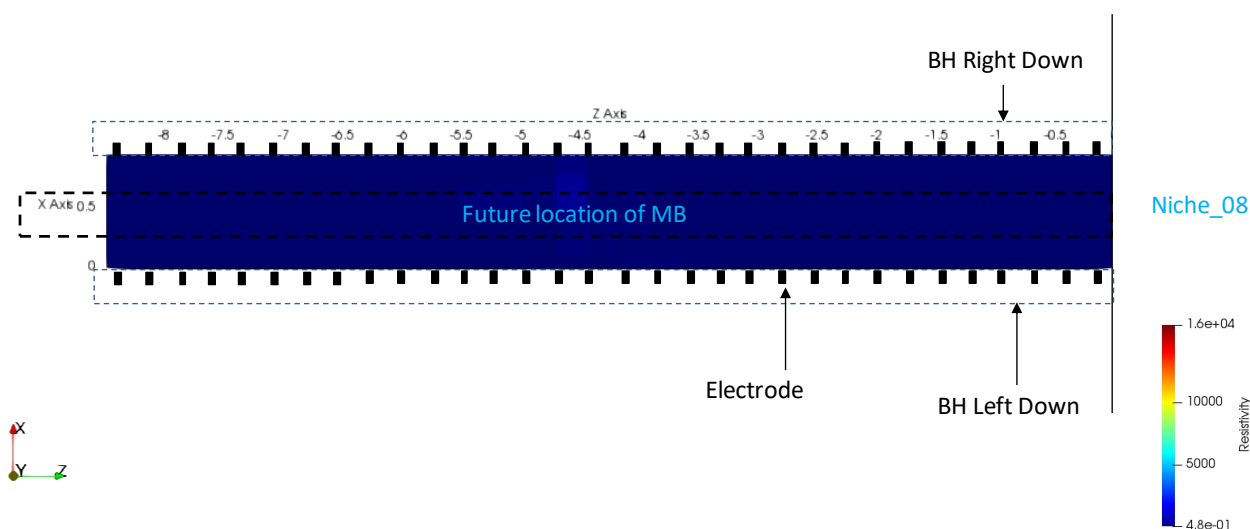

Figure 5: Cross section view of inversion results from survey T1 (RMS = 10.7%)

Figure 6 and Figure 7 show the ERT inversion of survey T2 performed during the monitoring stage in late September 2018 after curing of cement plug. Survey T2 distinguishes well the area of the cement plug and the bentonite. The data for T2 survey were processed, treated in terms of contact resistance, stacking errors and reciprocal errors and inverted.
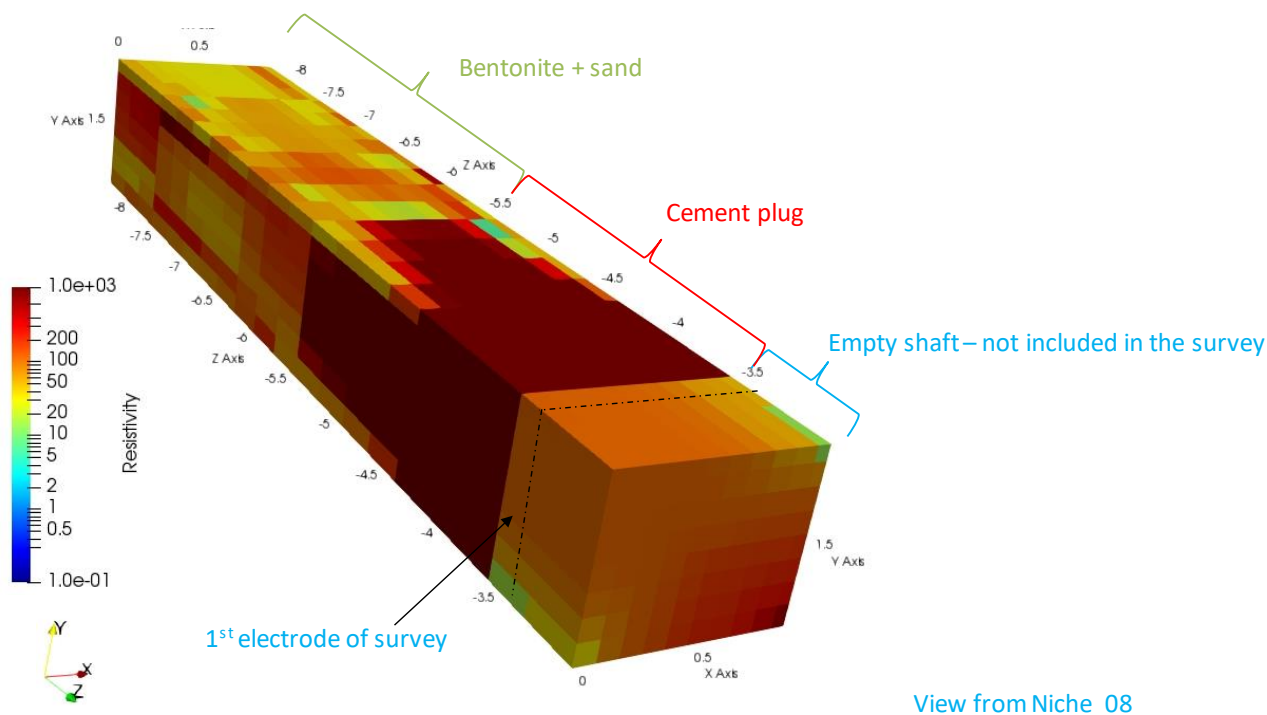

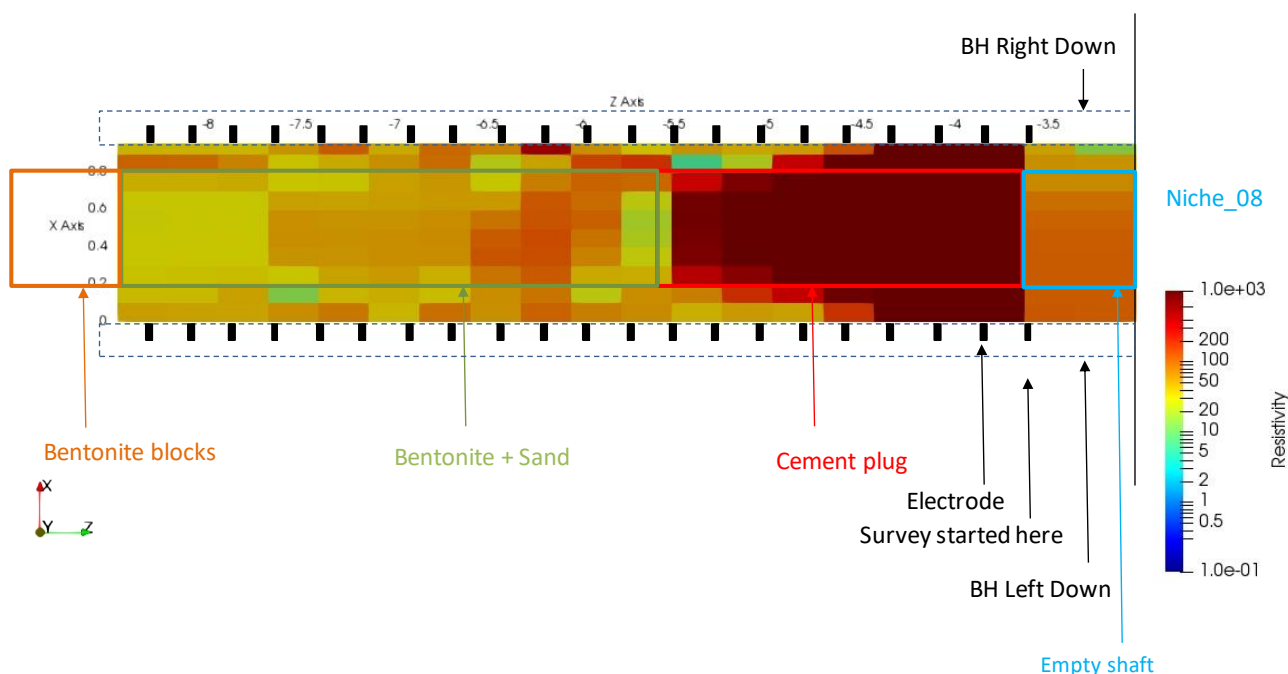*Figure 6: 3D view of inversion results from survey T2 (RMS = 5.16%)*

Figure 7: Cross section view of inversion results from survey T2 (RMS = 5.16%)

4. Discussion

4.1. ERT experiment

A considerable number of negative apparent resistivity data were collected during survey S2. This negative apparent resistivity does not appear to be real, since virtually no negative apparent resistivity remained after filtering the data according to the data quality procedure (Figure 8). However, it was evident that the protocol used for data collection during survey S2 was not appropriate since 46% of the total number of data collected were removed during the filtering stage and still the Root Mean Square (RMS) error of this inversion survey was 12.7%. Since then studies have been performed using forward modelling and sensitivity analysis to improve the protocol used for data collection.
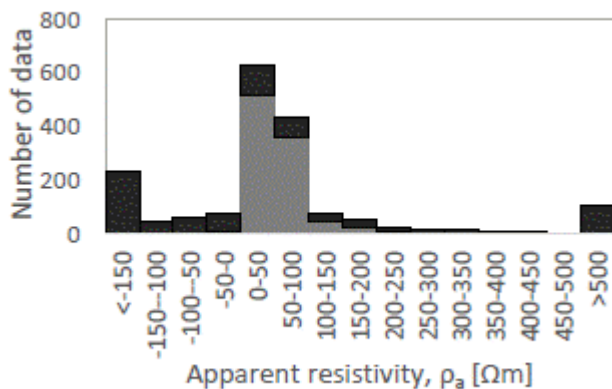

Figure 8: *Distribution of apparent resistivity before and after filtering out measurements associated with large geometric factors (black and grey bars, respectively) for survey S2.*

Survey S6 benefitted from the new improved protocol. For this survey only 16.5% of the total data collected have been filtered and the RMS obtained was 1.1%. Survey S6 happened 8 days after 26.06L of water had been injected into mat 1 (front of buffer), heater was set at 50°C (rear of buffer) and the temperature recorded by temperature sensors was stable for about 3 days. No changes are noticeable around the rear of the model and it is to be expected as the model only goes around depth 8.65m and the significant temperature change occurred between 8.9 and 9.1m (Figure 9).
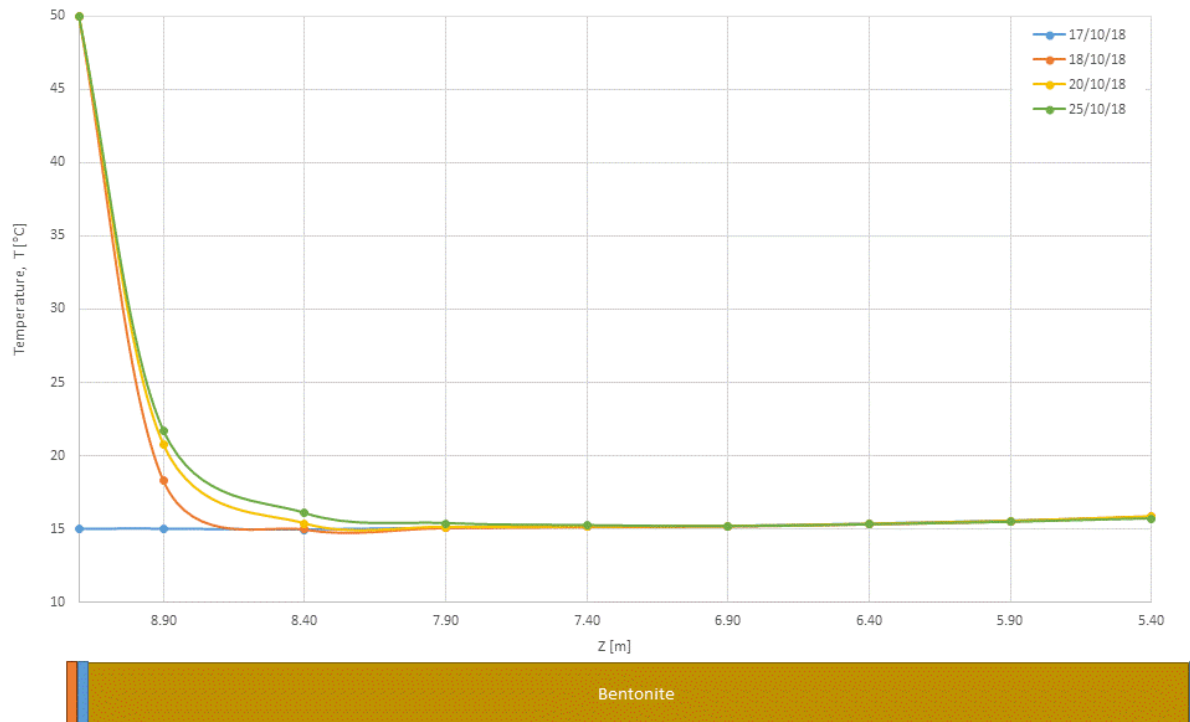
Figure 9:Temperature evolution recorded by temperature sensors installed along the buffer.

In the resistivity model (Figure 3) around the interface between the cement plug and the bentonite, there is a gradual reduction in resistivity. A TDR sensor (E1) located at Z=5.47m appears to be affected by water (resistivity drops recorded by this sensor during these 8 days after water injection) it is reasonable to assume that water has travel from mat 1 (5.1m) up until at least 5.4m depth, which is nicely characterised in the model of survey S6 by a drop in resistivity.

4.2. LTRBM

Measurements for survey T1 were collected in two ways: (1) each electrode in the quadripole was located into one borehole. For instance, the first quadripole of the surface protocol are electrodes 1, 17, 49 and 33, which means that current electrode A is electrode number 1, located in Borehole Left Up (LU); the other current electrode, B, is electrode number 17, located in Borehole Right Up (RU); potential electrode M is electrode number 49, located in Borehole Left Down (LD); and the other potential electrode, N, is number 33, located in Borehole Right Down (RD). (2) in a cross-borehole format where electrodes A and M are in one borehole and electrodes B and N are in the opposite borehole. Although the results obtained were reasonable and RMS error was within acceptable levels, it was clear that an improvement in the protocol was needed.

Thus, studies have been performed using forward modelling and sensitivity analysis to improve the protocol used for data collection in 3D for LTRBM, as well as collection of reciprocal measurements to ensure good data quality. The benefits of the use of the new improved protocol can be noted by the decrease of RMS error for survey T2.

5. Conclusion

Results of preliminary surveys carried out on both experiments confirmed that the resistivity of the host rock around both experiments area is quite homogenous and lower than 100Ωm in accordance with independent measurements carried out in previous campaigns [46]. In addition, the lesson learned from the blank tests allowed identifying key requirements for effective ERT measurements. These include, bespoke measurement protocols designed on the basis of the sensitivity analysis of the geometric factor and the collection of reciprocal data for enhanced data quality control.

Preliminary results of the monitoring period for both experiments are also promising, different materials within the installation are identifiable and changes in resistivity due to water injection and temperature increase are also expected to be noticeable.

The methodology developed for the electrode installation in boreholes and based on the use of PVC half tubes pushed against the borehole wall by inflatable pipes has proved to be successful. However, electrode contact resistance remains a challenge that needs to be addressed.

Interpretation of resistivity results could benefit from time-lapse inversions, which are not currently possible. Res3DInv software used for the 3D inversions does not offer the time-lapse option. Res2DInv does offer time-lapse option but to be able to do that the protocol used by all surveys have to be the same, which is not a possibility since different protocols were used for surveys S1, S2 and S3. Time-lapse analyses are still possible if a different software package is used for inversion and a different time-lapse approach is used based on the model mesh rather than protocols.

Electrical resistivity tomography has been successfully used for several years to monitor, qualitatively, changes in electrical resistivity of materials. Several features of the material (e.g. water content and temperature) are intrinsically sensitive to changes in electrical resistivity and thus could be connected and determined qualitatively by ERT surveys. At this qualitative level, the ERT is at technology readiness level (TRL) 9. The TRL of the ERT approach described here is at level 6. Research is still under development to (1) establish a semi-qualitative relationship between the resistivity measured in the tomography surveys and the resistivity of the material at control laboratory conditions and (2) determine the ideal characteristics of the less-intrusive scenario for EBS monitoring.

6. Acknowledgements

References

1.   J. D. Bredehoeft, A. W. England, D. B. Stewart, N. J. Trask, & I. J. Winograd, *Geologic Disposal of High-Level Radioactive Wastes- Earth-Science Perspectives* (1978).

2.   M. White, J. Farrow, & M. Crawford, *Deliverable D2.1 : Repository Monitoring Strategies and Screening*

Methodologies (2017).

3. P. Cosenza, A. Ghorbani, N. Florsch, & A. Revil, Effects of drying on the low-frequency electrical properties of Tournemire argillites. *Pure and Applied Geophysics*, **164** (2007) 2043–2066. https://doi.org/10.1007/s00024-007-0253-0.

4. B. E. Danielsen & T. Dahlin, Numerical modelling of resolution and sensitivity of ERT in horizontal boreholes. *Journal of Applied Geophysics*, **70** (2010) 245–254. https://doi.org/10.1016/j.jappgeo.2010.01.005.

5. T. Hermans, S. Wildemeersch, P. Jamin, P. Orban, S. Brouyère, A. Dassargues, & F. Nguyen, Quantitative temperature monitoring of a heat tracing experiment using cross-borehole ERT. *Geothermics*, **53** (2015) 14–26. https://doi.org/10.1016/j.geothermics.2014.03.013.

6. S. A. Korteland & T. Heimovaara, Quantitative inverse modelling of a cylindrical object in the laboratory using ERT: An error analysis. *Journal of Applied Geophysics*, **114** (2015) 101–115. https://doi.org/10.1016/j.jappgeo.2014.10.026.

7. A. J. Merritt, J. E. Chambers, P. B. Wilkinson, L. J. West, W. Murphy, D. Gunn, & S. Uhlemann, Measurement and modelling of moisture-electrical resistivity relationship of fine-grained unsaturated soils and electrical anisotropy. *Journal of Applied Geophysics*, **124** (2016) 155–165. https://doi.org/10.1016/j.jappgeo.2015.11.005.

8. A. M. Carey, G. B. Paige, B. J. Carr, & M. Dogan, Forward modeling to investigate inversion artifacts resulting from time-lapse electrical resistivity tomography during rainfall simulations. *Journal of Applied Geophysics*, **145** (2017) 39–49. https://doi.org/10.1016/j.jappgeo.2017.08.002.

9. J. Wang, X. Zhang, & L. Du, A laboratory study of the correlation between the thermal conductivity and electrical resistivity of soil. *Journal of Applied Geophysics*, **145** (2017) 12–16. https://doi.org/10.1016/j.jappgeo.2017.07.009.

10. O. A. L. de Lima, H. K. Sato, & M. J. Porsani, Imaging industrial contaminant plumes with resistivity techniques. *Journal of Applied Geophysics*, **34** (1995) 93–108. https://doi.org/10.1016/0926-9851(95)00014-3.

11. D. J. LaBrecque, A. L. Ramirez, W. D. Daily, A. M. Binley, & S. A. Schima, ERT monitoring of environmental remediation processes. *Measurement Science and Technology*, **7** (1996) 375–383. https://doi.org/10.1088/0957-0233/7/3/019.

12. A. K. Benson, K. L. Payne, & M. A. Stubben, Mapping groundwater contamination using dc resistivity and VLF geophysical methods–A case study. *Geophysics*, **62** (1997) 80–86. https://doi.org/10.1190/1.1444148.

13. P. Martinez-Pagan, A. Faz, & E. Aracil, The use of 2D electrical tomography to assess pollution in slurry ponds of the Murcia region, SE Spain. *Near Surface Geophysics*, **7** (2009) 49–61. https://doi.org/10.3997/1873-0604.2008033.

14. J. Deceuster, O. Kaufmann, & M. Van Camp, Automated identification of changes in electrode contact properties for long-term permanent ERT monitoring experiments. *Geophysics*, **78** (2013) E79–E94. https://doi.org/10.1190/GEO2012-0088.1.

15. D. Ntarlagiannis, J. Robinson, P. Soupios, & L. Slater, Field-scale electrical geophysics over an olive oil mill waste deposition site: Evaluating the information content of resistivity versus induced polarization (IP) images for delineating the spatial extent of organic contamination. *Journal of Applied Geophysics*, **135** (2016) 418–426. https://doi.org/10.1016/j.jappgeo.2016.01.017.

16. D. F. Rucker, M. T. Levitt, & W. J. Greenwood, Three-dimensional electrical resistivity model of a nuclear waste disposal site. *Journal of Applied Geophysics*, **69** (2009) 150–164. https://doi.org/10.1016/j.jappgeo.2009.09.001.

17. P. Sentenac & M. Zielinski, Clay fine fissuring monitoring using miniature geo-electrical resistivity arrays. *Environmental Earth Sciences*, **59** (2009) 205–214. https://doi.org/10.1007/s12665-009-0017-5.

18. G. Jones, M. Zielinski, & P. Sentenac, Mapping desiccation fissures using 3-D electrical resistivity tomography. *Journal of Applied Geophysics*, **84** (2012) 39–51. https://doi.org/10.1016/j.jappgeo.2012.06.002.

19. G. Jones, P. Sentenac, & M. Zielinski, Desiccation cracking detection using 2-D and 3-D Electrical Resistivity Tomography : Validation on a fl ood embankment. *Journal of Applied Geophysics*, **106** (2014) 196–211. https://doi.org/10.1016/j.jappgeo.2014.04.018.

20. S. Banham & J. K. Pringle, Geophysical and intrusive site investigations to detect an abandoned coal-mine access shaft, Apedale, Staffordshire, UK. *Near Surface Geophysics*, **9** (2011) 483–496.

21. N. Tonkov & M. H. Loke, A resistivity survey of a burial mound in the "Valley of the Thracian Kings." *Archaeological Prospection*, **13** (2006) 129–136. https://doi.org/10.1002/arp.273.

22. B. Ullrich, T. Guenther, & C. Ruecker, Electrical Resistivity Tomography Methods for Archaeological Prospection. *Geophysical Prospecting*, (2007) 1–7.

23. S. Negri, G. Leucci, & F. Mazzone, High resolution 3D ERT to help GPR data interpretation for researching archaeological items in a geologically complex subsurface. *Journal of Applied Geophysics*, **65** (2008) 111–120. https://doi.org/10.1016/j.jappgeo.2008.06.004.

24. G. Leucci & F. Greco, 3D ERT Survey to Reconstruct Archaeological Features in the Subsoil of the " Spirito Santo " Church Ruins at the Site of Occhiolà (Sicily , Italy). *Archaeology*, **1** (2012) 1–6. https://doi.org/10.5923/j.archaeology.20120101.01.

25. G. V. Ganerød, J. S. Rønning, E. Dalsegg, H. Elvebakk, K. Holmøy, B. Nilsen, & A. Braathen, Comparison of geophysical methods for sub-surface mapping of faults and fracture zones in a section of the Viggja road tunnel, Norway. *Bulletin of Engineering Geology and the Environment*, **65** (2006) 231–243. https://doi.org/10.1007/s10064-006-0041-6.

26. K. Ramachandran, B. Tapp, T. Rigsby, & E. Lewallen, Imaging of fault and fracture controls in the arbuckle-simpson aquifer, Southern Oklahoma, USA, through electrical resistivity sounding and tomography methods. *International Journal of Geophysics*, (2012) 1–10. https://doi.org/10.1155/2012/184836.

27. A. A. Aning, P. Tucholka, & S. K. Danuor, 2D Electrical Resistivity Tomography (ERT) Survey using the Multi-Electrode Gradient Array at the Bosumtwi Impact Crater ,. **3** (2013) 12–27.

28. W. Daily & E. Owen, Cross-borehole resistivity tomography. *Geophysics*, **56** (1991) 1228–1235.

29. W. Daily, A. Ramirez, D. LaBrecque, & W. Barber, Electrical resistance tomography experiments at the Oregon Graduate Institute. *Journal of Applied Geophysics*, **33** (1995) 227–237. https://doi.org/10.1016/0926-9851(95)90043-8.

30. D. LaBrecque, M. Miletto, W. Daily, A. Ramirez, & E. Owen, The effects of noise on Occam's inversion of resistivity tomography data. *Geophysics*, **61** (1996) 538–548.

31. H. K. French, C. Hardbattle, A. Binley, P. Winship, & L. Jakobsen, Monitoring snowmelt induced unsaturated flow and transport using electrical resistivity tomography. *Journal of Hydrology*, **267** (2002) 273–284. https://doi.org/10.1016/s0022-1694(02)00156-7.

32. R. Guérin, Borehole and surface-based hydrogeophysics. *Hydrogeology Journal*, **13** (2005) 251–254. https://doi.org/10.1007/s10040-004-0415-4.

33. J. Deceuster, J. Delgranche, & O. Kaufmann, 2D cross-borehole resistivity tomographies below foundations as a tool to design proper remedial actions in covered karst. *Journal of Applied Geophysics*, **60** (2006) 68–86. https://doi.org/10.1016/j.jappgeo.2005.12.005.

34. P. B. Wilkinson, P. I. Meldrum, O. Kuras, J. E. Chambers, S. J. Holyoake, & R. D. Ogilvy, High-resolution Electrical Resistivity Tomography monitoring of a tracer test in a confined aquifer. *Journal of Applied Geophysics*, **70** (2010) 268–276. https://doi.org/10.1016/j.jappgeo.2009.08.001.

35.   A. Denis, A. Marache, T. Obellianne, & D. Breysse, Electrical resistivity borehole measurements: Application to an urban tunnel site. *Journal of Applied Geophysics*, **50** (2002) 319–331. https://doi.org/10.1016/S0926-9851(02)00150-7.

36.   C. Oberdörster, J. Vanderborght, A. Kemna, & H. Vereecken, Investigating Preferential Flow Processes in a Forest Soil Using Time Domain Reflectometry and Electrical Resistivity Tomography. *Vadose Zone Journal*, **9** (2010) 350–361. https://doi.org/10.2136/vzj2009.0073.

37.   I. Coscia, S. A. Greenhalgh, N. Linde, J. Doetsch, L. Marescot, T. G nther, T. Vogt, & A. G. Green, 3D crosshole ERT for aquifer characterization and monitoring of infiltrating river water. *Geophysics*, **76** (2011) G49–G59. https://doi.org/10.1190/1.3553003.

38.   X. Yang, R. N. Lassen, K. H. Jensen, & M. C. Looms, Monitoring CO2migration in a shallow sand aquifer using 3D crosshole electrical resistivity tomography. *International Journal of Greenhouse Gas Control*, **42** (2015) 534–544. https://doi.org/10.1016/j.ijggc.2015.09.005.

39.   C. Schmidt-Hattenberger, P. Bergmann, T. Labitzke, F. Wagner, & D. Rippe, Permanent crosshole electrical resistivity tomography (ERT) as an established method for the long-term CO2monitoring at the Ketzin pilot site. *International Journal of Greenhouse Gas Control*, **52** (2016) 432–448. https://doi.org/10.1016/j.ijggc.2016.07.024.

40.   T. Rothfuchs, R. Miehe, H. Moog, & K. Wieczorek, *Geoelectric Investigation of Bentonite Barrier Saturation* (2004).

41.   M. Furche & K. Scuster, *Long-term performance of engineered barrier systems PEBS* (2014).

42.   B. Garitte, H. Weber, & H. R. Müller, *Requirements, manufacturing and QC of the buffer components Report LUCOEX – WP2* (2015).

43.   B. de C. F. L. Lopes, C. Sachet, P. Sentenac, V. Benes, P. Dick, J. Bertrand, & A. Tarantino, Preliminary non-intrusive geophysical electrical resistivity tomography surveys of a mock-up scale monitoring of an engineered barrier system at URL Tournemire. *Geological Society - Multiples Roles of Clays in Radioactive Waste Confinement*, **482** (2018). https://doi.org/10.1144/SP482.11.

44.   M. H. Loke, RES2DINV. Rapid 2-D Resistivity & IP inversion using the least-squares method. (2015) 127P.

45.   M. H. Loke, *Rapid 3-D Resistivity & IP inversion using the least-squares method* (2017).

46.   C. Gélis, M. Noble, J. Cabrera, S. Penz, H. Chauris, & E. M. Cushing, Ability of High-Resolution Resistivity Tomography to Detect Fault and Fracture Zones: Application to the Tournemire Experimental Platform, France. *Pure and Applied Geophysics*, **173** (2016) 573–589. https://doi.org/10.1007/s00024-015-1110-1.